

## EXPLOSIVE YIELDS OF MASSIVE STARS FROM $Z = 0$ TO $Z = Z_{\odot}$

ALESSANDRO CHIEFFI<sup>1,2,3</sup> AND MARCO LIMONGI<sup>2,3,4</sup>

Received 2003 November 7; accepted 2004 February 25

### ABSTRACT

We present a new and homogeneous set of explosive yields for masses 13, 15, 20, 25, 30, and 35  $M_{\odot}$  and metallicities  $Z = 0, 10^{-6}, 10^{-4}, 10^{-3}, 6 \times 10^{-3},$  and  $2 \times 10^{-2}$ . A wide network extending up to Mo has been used in all computations. We show that at low metallicities ( $Z \leq 10^{-4}$ ), the final yields do not depend significantly on the initial chemical composition of the models, so a scaled solar distribution may be safely assumed at all metallicities. Moreover, no elements above Zn are produced by any mass in the grid up to a metallicity  $\sim 10^{-3}$ . These yields are available for any choice of the mass cut on request.

*Subject headings:* nuclear reactions, nucleosynthesis, abundances — stars: evolution — supernovae: general

*On-line materials:* color figure, machine-readable table

### 1. INTRODUCTION

A proper understanding of the chemical evolution of our Galaxy and of the universe in general requires good knowledge of the chemical composition of the matter ejected by stars of different masses and initial composition. Massive stars certainly play a pivotal role in the chemical enrichment of the interstellar medium, because they are very probably responsible for the production of at least most of the intermediate-mass elements (O–Ca). In spite of their central role in the general understanding of the chemical evolution of matter, only one extended set of models has been published so far: the one computed and discussed by Woosley & Weaver (1995, hereafter WW95) and Timmes et al. (1995, hereafter TWW95). Their yields are based on presupernova models computed by assuming, among others, no mass loss, no rotation, a moderate amount of overshooting and semiconvection, a value of  $^{12}\text{C}(\alpha, \gamma)^{16}\text{O}$  calibrated on preexplosive yields, and a network extending up to Ge. The explosions were computed in spherical symmetry, and the yields eventually obtained by imposing on the ejecta a specific final kinetic energy (their cases A, B, and C). The initial chemical composition of the models at intermediate metallicities was obtained from a galactic chemical evolution model (described by TWW95).

Unfortunately, present simulations of both the presupernova evolution and the explosion are still far from being robustly established. Qualitatively (and partly quantitatively) we know how and where the various nuclei are synthesized (see, e.g., WW95; Arnett 1996; Thielemann et al. 1996; Limongi et al. 2000), but still large uncertainties connected to both the hydrostatic evolution and the explosion of massive stars prevent a rigorous computation of the yields. Such uncertainties are mainly related to the efficiency of the convection (see, e.g., Chiosi & Maeder 1986; Woosley & Weaver 1988; Bazan &

Arnett 1994), the determination of the cross section of a few nuclear processes [first,  $^{12}\text{C}(\alpha, \gamma)^{16}\text{O}$ ; see, e.g., Weaver & Woosley 1993; Imbriani et al. 2001], the time delay between the collapse of the core and the rejuvenation of the shock wave, and the precise location of the mass cut (which is the mass coordinate that separates the part of the star that collapses in the remnant from the one that is ejected outward), even in spherical symmetry. To further complicate the situation, rotation, mass loss, magnetic field, and asymmetric explosions may also produce large variations in the final yields (see, e.g., Heger et al. 2000; Maeda & Nomoto 2003).

Some years ago we began a long-term project devoted to the study of the evolution of massive stars and their associated explosive yields (Chieffi et al. 1998; Limongi et al. 2000; Limongi & Chieffi 2002, 2003, hereafter LC03; Chieffi & Limongi 2002). Since the beginning, we made a strong effort to avoid using the various kinds of statistical equilibrium usually adopted to determine the chemical evolution of the matter at temperatures larger than roughly 3 billion degrees. Moreover, we made an effort to fully couple the integration of the physical equations to those that describe the evolution of the nuclear species in order to increase the numerical accuracy. Over the years, we progressively increased the nuclear network, which now extends up to molybdenum. However, like WW95, our models are still computed by neglecting both mass loss and rotation. In our latest paper of the series (LC03), we presented our most updated version of the hydrostatic code (FRANEC) together with our new hydrodynamic code needed to follow the propagation of the blast wave. We also showed that the yields produced by a given stellar mass depend mainly on the location of the mass cut rather than the explosion energy. This means that as a first approximation, the yields corresponding to the ejection of different amounts of  $^{56}\text{Ni}$  may be obtained by assuming an explosion strong enough to eject the full mantle and imposing the mass cut at the desired  $^{56}\text{Ni}$  abundance by hand. Such a finding means that one can easily explore different choices for the mass cut without the necessity of recomputing the explosion of the models many times.

By making use of the latest versions of the two codes (hydrostatic and hydrodynamic) described in LC03, we present a wide database of yields. In particular, we present the explosive yields produced by a grid of six masses (13, 15, 20, 25, 30, and 35  $M_{\odot}$ ) and six metallicities ( $Z = 0, 10^{-6}, 10^{-4}, 10^{-3}, 6 \times 10^{-3},$  and  $2 \times 10^{-2}$ ).

<sup>1</sup> Istituto di Astrofisica Spaziale e Fisica Cosmica (CNR), Via Fosso del Cavaliere, I-00133 Roma, Italy; achieffi@rm.iasf.cnr.it.

<sup>2</sup> School of Mathematical Sciences, P.O. Box 28M, Monash University, Victoria 3800, Australia.

<sup>3</sup> Centre for Astrophysics and Supercomputing, Swinburne University of Technology, Mail Number 31, P.O. Box 218, Hawthorn, Victoria 3122, Australia.

<sup>4</sup> Istituto Nazionale di Astrofisica–Osservatorio Astronomico di Roma, Via Frascati 33, I-00040 Monteporzio Catone, Italy; marco@mporzio.astro.it.

The paper is organized as follows. The evolutionary code and the input physics adopted to compute the grid are briefly summarized in § 2. Section 3 is devoted to the discussion of the initial chemical composition used to compute the models in the intermediate metallicity range between the primordial and the solar one. A final discussion and conclusions follow.

## 2. HYDROSTATIC AND HYDRODYNAMIC CODES

The presupernova evolutions have been computed by means of the latest version of the FRANEC code, which has been described in LC03 (and references therein). We just recall here that the nuclear network extends up to molybdenum and includes 40 isotopes (from neutrons to  $^{30}\text{Si}$ ) in hydrogen burning, 149 isotopes (from neutrons to  $^{98}\text{Mo}$ ) in helium burning, and 267 isotopes (from neutrons to  $^{98}\text{Mo}$ ) in all of the more advanced burning phases. In total, 282 isotopes (see Table 1 in LC03) and about 3000 reaction rates were explicitly included in the various nuclear burning stages. The nuclear network is fully coupled to the equations describing the physical structure of the star, so that both the physical and chemical evolution due to the nuclear reactions are solved simultaneously. No nuclear statistical equilibrium approximation has been adopted at high temperatures.

The explosive nucleosynthesis associated with the explosion of each massive star model is computed with the same procedure described in LC03. The propagation of the shock front through the mantle of the star is followed by solving the hydrodynamic equations in spherical symmetry and Lagrangian form, following the prescription of Richtmeyer & Morton (1967) and Mezzacappa & Bruenn (1993). The chemical evolution of the matter is computed by coupling the same nuclear network adopted in the hydrostatic calculations (Table 1 of LC03) to the hydrodynamic equations. The explosion is started by imparting an initial velocity  $v_0$  to a mass coordinate of  $\simeq 1 M_\odot$  of the presupernova model, i.e., well inside the iron core, and by imposing the inner edge of the exploding mantle to move on a ballistic trajectory under the gravitational field of the compact remnant. The initial velocity  $v_0$  is properly tuned in order to eject all the mass above the Fe core. By taking advantage of the fact that the final yields mainly depend on the mass cut location (see LC03), yields corresponding to different amounts of  $^{56}\text{Ni}$  ejected are then easily obtained by fixing the mass cut by hand a posteriori.

## 3. THE INITIAL COMPOSITION OF THE STELLAR MODELS

We computed the presupernova evolution of the six massive star models for various metallicities ranging from zero to solar. The zero metallicity models were computed by assuming an initial primordial composition ( $Z = 0$ ,  $Y = 0.23$ ), while the solar metallicity models were computed starting with a scaled solar heavy elements distribution, as derived from Anders & Grevesse (1989), and an initial helium mass fraction  $Y = 0.285$ . The initial chemical composition adopted between these two extreme metallicities requires some discussion. In general, the initial composition of a star of a given metallicity is the result of the enrichment of the interstellar medium provided by previous stellar generations; hence, its determination would involve a Galactic chemical evolution (GCE) model and would therefore depend on the initial mass function (IMF), star formation rate, infall, chemical yields, etc. Such an auto-consistent procedure has been adopted by WW95 and TWW95 to determine the initial chemical composition of the models of

intermediate metallicities ( $0 < Z < Z_\odot$ ). Unfortunately, models computed in this way are obviously strictly linked to the GCE model to which they belong and should not be used in any other GCE simulation. Hence, the computation of the stellar models, and their associated explosive yields, should be redone for any GCE simulation, and such a procedure would obviously require an enormous amount of computer time. It is therefore crucial to understand whether it is possible to compute a grid of explosive yields of *general* purpose and, obviously, which is the initial chemical composition that should be used; in the following, we will address such a problem.

In order to study how (and if) the specific abundances of the various nuclei affect the final yields, we performed two test evolutions of a  $25 M_\odot$  model having an initial global metallicity  $Z = 10^{-4}$ . We chose this metallicity because the largest deviations from a scaled solar distribution occur at low metallicities. In the first test, we started from a scaled solar distribution and set to zero the abundances of all the nuclei but  $^{12}\text{C}$ ,  $^{14}\text{N}$ ,  $^{16}\text{O}$ , and  $^{56}\text{Fe}$ . Figure 1 (*top panel*) shows the logarithmic ratio between the yields obtained in the test case and the standard ones (i.e., those obtained with a scaled solar composition). It is quite evident that the two sets are in very good agreement. Co is the only element different by a factor of 2. This test clearly demonstrates that the initial abundances of the elements initially set to zero do not significantly influence the final explosive yields. Hence, for the sake of simplicity, we can adopt a scaled solar distribution for all of them.

The next step is to understand how (and if) the initial abundances of the CNO nuclei affect the final yields. Hence, we performed a second test in which, starting from a scaled solar distribution, we imposed an  $[\text{O}/\text{Fe}]$  equal to 0.4 dex and a global metallicity  $Z = 10^{-4}$ . Obviously, this test automatically includes a possible variation of the initial abundances of C and/or N, because the initial relative abundances among the CNO nuclei are promptly brought to their equilibrium values as soon as the star settles on the main sequence. This test is also particularly interesting because the global abundance of CNO controls the size of the H convective core and is the starting point of the important chain,  $^{14}\text{N}(\alpha, \gamma)^{18}\text{F}(\beta^+)^{18}\text{O}(\alpha, \gamma)^{22}\text{Ne}(\alpha, n)^{25}\text{Mg}$ , which is a very important neutron source. Figure 1 (*bottom panel*) shows the logarithmic ratio between the yields obtained in the test and in the standard cases; once again, the two sets of yields are in good agreement (within a factor of 2) even if a few elements now show some differences (largely confined, however, within a factor of 4): N, F, K, Sc, Cu, and Zn. N is a typical product of the H burning, and its final yield depends directly on the initial CNO abundance. Hence, it is quite obvious that a scaled solar distribution cannot provide the same yield provided by an initial CNO-enhanced composition. However, since massive stars are probably not the main contributors to the N production in the Galaxy, the adoption of an initial scaled solar abundance for N does not constitute too serious a problem. F is probably mostly produced by the neutrino-induced reactions during the explosion (WW95). Since these processes are not presently included in our models, our current yield for F is not very reliable in any case. In addition, the differences obtained for K, Sc, Cu, and Zn should not be considered a big problem, because in any case, their production relies completely on the location of the mass cut (the mass location that divides the part of the star that eventually collapses in the remnant from that which is expelled outward), which is still a very uncertain theoretical prediction. Hence, waiting for yields based on more reliable explosive models, we conclude that at present

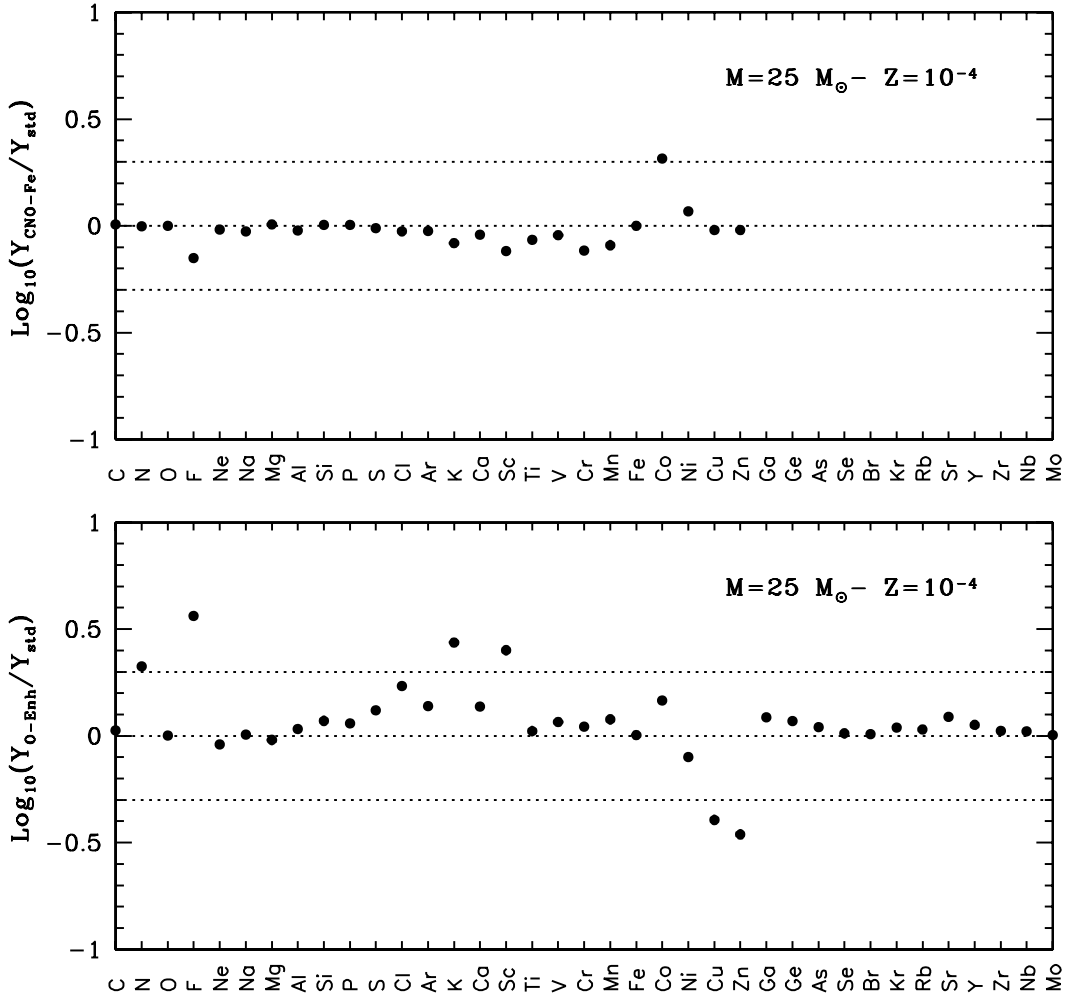


FIG. 1.—*Top*: Logarithmic ratio between the explosive yields produced by  $25 M_{\odot}$  of global metallicity  $Z = 10^{-4}$  in which the initial abundances of all the nuclei are set to zero, except  $^{12}\text{C}$ ,  $^{14}\text{N}$ ,  $^{16}\text{O}$ , and  $^{56}\text{Fe}$ , and those produced by a standard  $25 M_{\odot}$  having an initial scaled solar metallicity of  $Z = 10^{-4}$ . *Bottom*: Logarithmic ratio between the explosive yields produced by  $25 M_{\odot}$  of global metallicity  $Z = 10^{-4}$  and  $[\text{O}/\text{Fe}] = 0.4$ , and those produced by the standard reference model.

the adoption of an initial scaled solar distribution of all the elements relative to Fe is a reasonable compromise between generality and accuracy. Therefore, in the following we assume a scaled solar distribution (Anders & Grevesse 1989) for all the metallicities higher than zero.

The weak dependence of the *elemental* yields on the initial chemical composition obtained above is not surprising, because the most abundant isotope of each even element is of primary origin (explosive and/or hydrostatic), while the odd elements are always produced by a combination of a primary and a secondary component; as the metallicity lowers, the secondary component drops to zero, but the primary one remains obviously active. It goes without saying, at this point, that such findings also justify (a posteriori) the use of the WW95 yields in GCE simulations other than that (TWW95) from which they come.

The grid of initial metallicities we eventually chose is  $(Z, Y) = (0, 0.23)$ ,  $(10^{-6}, 0.23)$ ,  $(10^{-4}, 0.23)$ ,  $(10^{-3}, 0.23)$ ,  $(6 \times 10^{-3}, 0.26)$ , and  $(2 \times 10^{-2}, 0.285)$ , where  $Z$  represents the global metallicity and  $Y$  represents the initial  $^4\text{He}$  mass fraction.

#### 4. DISCUSSION AND CONCLUSIONS

The final explosive isotopic yields in solar masses of all the computed models are reported in Table 1, available in

electronic format (a stub version is available in print format), once all the unstable isotopes have decayed into their stable isobars. The yields of selected radioactive isotopes at  $10^7$  s after the explosion are collected in the same table. For obvious reasons, we could not present different sets of yields for different choices of the mass cut; hence, we chose to present just one case, i.e., the one in which all masses eject  $0.1 M_{\odot}$  of  $^{56}\text{Ni}$ . Any other choice is promptly available on request.

The full set of elemental production factors (PFs) is shown in Figure 2. Each panel refers to a specific metallicity, and each symbol refers to a given mass (see figure caption). We reiterate that, in our case, the PF of any given isotope/element is defined as the ratio of each isotope's/element's mass fraction in the total ejecta divided by its corresponding initial mass fraction, i.e.,  $\text{PF} = X_{\text{ejected}}/X_{\text{ini}}$ . Note that this definition is different from the one adopted by WW95, where  $\text{PF} = X_{\text{ejected}}/X_{\odot}$ .

Some basic properties of the present yields may be seen by looking at Figure 2. First, the PFs of all the elements from C to Zn decrease significantly as the metallicity increases, almost independent of the initial mass—the only exceptions being N and F. The reason for this is that, regardless of the mass of the star, the yields of the elements do not vary by more than an order of magnitude within the entire range of metallicities (see

TABLE 1  
EXPLOSIVE YIELDS

Mass	13 $M_{\odot}$	15 $M_{\odot}$	20 $M_{\odot}$	25 $M_{\odot}$	30 $M_{\odot}$	35 $M_{\odot}$
Metallicity ( $Z = 0$ )						
$M_{\text{ejected}}$ .....	11.79	13.53	18.33	23.40	27.93	32.97
$M_{\text{remnant}}$ .....	1.21	1.47	1.67	1.60	2.07	2.03
$^{56}\text{Ni}$ .....	0.0913	0.1000	0.1000	0.1000	0.1000	0.1000
$^1\text{H}$ .....	6.86(+00)	7.77(+00)	9.74(+00)	1.16(+01)	1.32(+01)	1.47(+01)
$^2\text{H}$ .....	6.55(-17)	5.95(-17)	6.34(-17)	1.77(-16)	9.76(-16)	3.05(-16)
$^3\text{He}$ .....	3.07(-05)	3.01(-05)	2.90(-05)	2.77(-05)	2.72(-05)	2.71(-05)
$^4\text{He}$ .....	4.05(+00)	4.65(+00)	6.26(+00)	7.78(+00)	9.33(+00)	1.07(+01)
$^6\text{Li}$ .....	5.22(-19)	1.16(-18)	3.20(-18)	1.88(-16)	6.86(-16)	1.73(-16)
$^7\text{Li}$ .....	4.15(-11)	1.19(-10)	2.16(-10)	2.40(-10)	2.60(-10)	2.42(-10)
$^9\text{Be}$ .....	1.15(-59)	1.33(-59)	1.80(-59)	4.11(-30)	5.25(-29)	2.89(-30)

NOTES.—Table 1 is published in its entirety in the electronic edition of the *Astrophysical Journal*. A portion is shown here for guidance regarding its form and content.

Table 1), while the  $X_{\text{ini}}$  obviously scale directly with the initial global metallicity and hence vary by several orders of magnitude. Such a strong dependence of the PFs on the metallicity simply means that the larger the metallicity, the more difficult the further chemical enrichment.

A second feature is the well-known *odd-even effect*; i.e., the difference between the PFs of the odd (Na–Sc) and the even nuclei (Ne–Ca) decreases as the metallicity increases: at the solar metallicity, most of the elements show a roughly scaled solar distribution (see LC03 for a more detailed discussion of

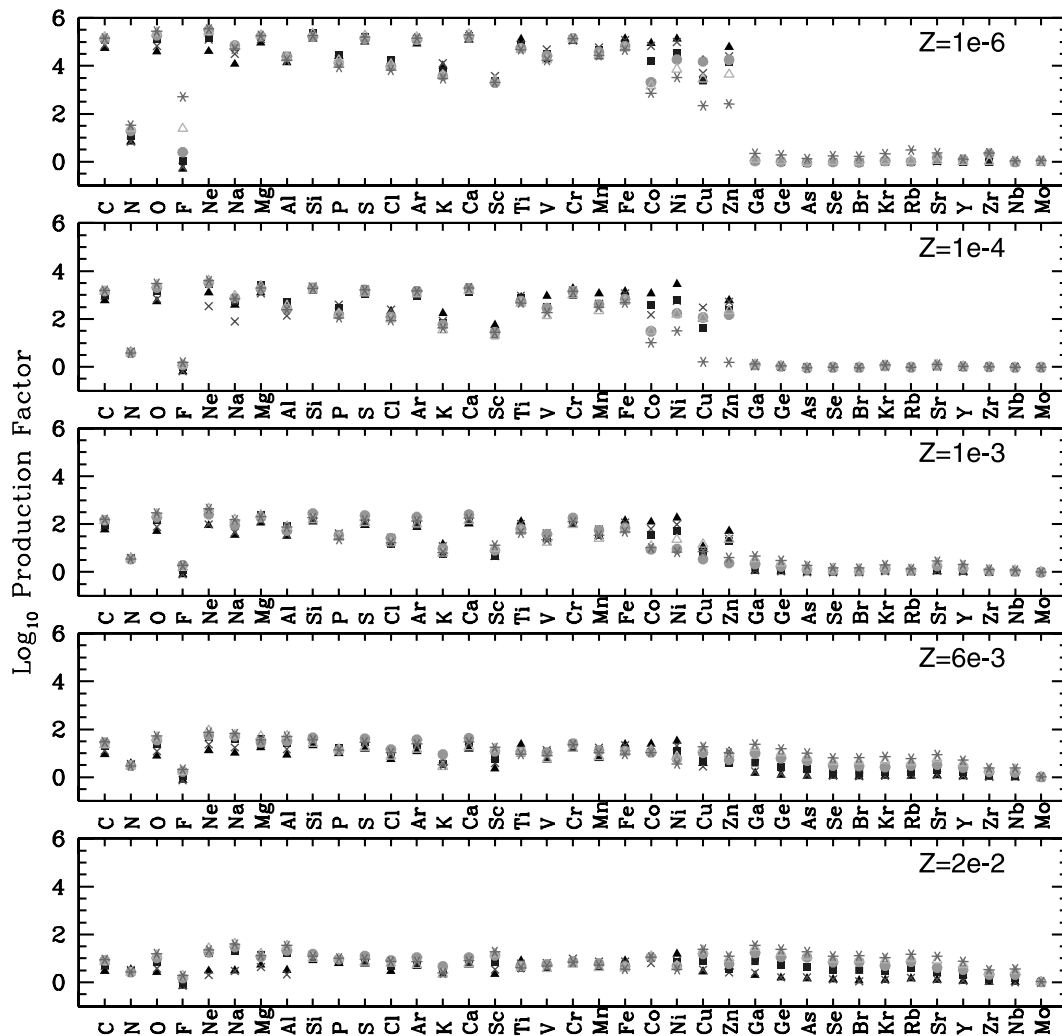


FIG. 2.—Production factors of all the elements from C to Mo. The symbols refer to the six masses: 13  $M_{\odot}$  (filled triangles), 15  $M_{\odot}$  (crosses), 20  $M_{\odot}$  (filled squares), 25  $M_{\odot}$  (filled circles), 30  $M_{\odot}$  (open triangles), and 35  $M_{\odot}$  (asterisks). Each panel refers to the metallicity reported in the top right corner. [See the electronic edition of the *Journal* for a color version of this figure.]

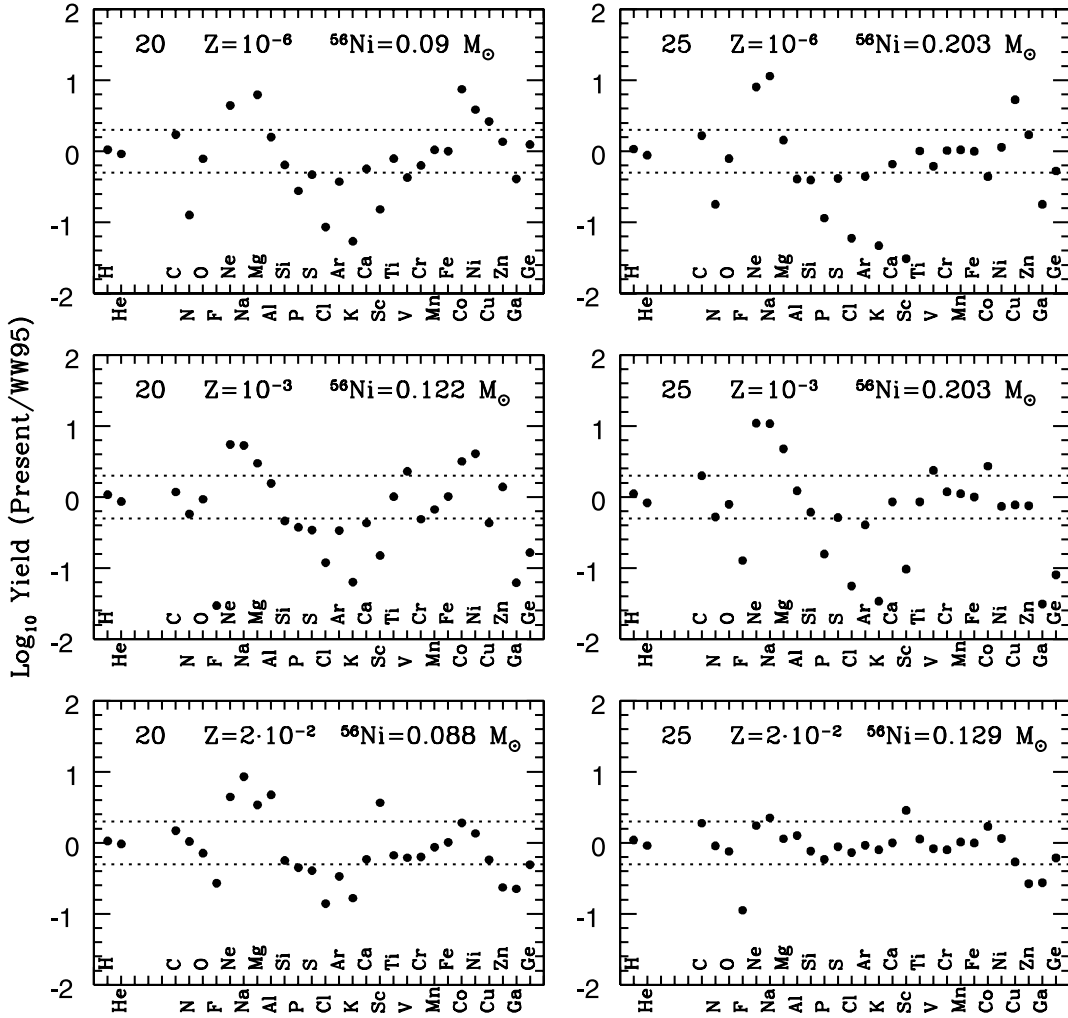


FIG. 3.—Comparison between the elemental yields provided by WW95 and the present ones for two masses, 20 and 25  $M_{\odot}$ , and for three selected metallicities,  $Z = 10^{-6}$  (top),  $Z = 10^{-3}$  (middle), and  $Z = 2 \times 10^{-2}$  (bottom).

this topic). It is worth noting that, with the  $^{12}\text{C}(\alpha, \gamma)^{16}\text{O}$  rate adopted in the present calculations, Ne, Mg, Si, S, Ar, and Ca preserve a scaled solar distribution at all metallicities (see Imbriani et al. 2001 for a more comprehensive discussion of this topic).

A last feature worth mentioning here is that below  $Z = 10^{-3}$ , there is a cutoff in the PFs at the level of Zn, i.e., no elements heavier than Zn are produced. On the contrary, above  $Z = 10^{-3}$ , such a cutoff progressively decreases so that a consistent production of elements beyond Zn is obtained. Elements above Sr are not produced in a significant amount even at solar metallicity. This means that the observed abundances of elements above Zn in very metal-poor stars must be attributed to stars (or, in general, to processes) outside the range presently analyzed.

Since the only other paper presenting a full set of yields is WW95, in Figure 3 we show the comparison between the WW95 and the present yields for two masses and three metallicities. Only elements up to Ge are shown, because the nuclear network adopted by WW95 does not extend above this element. For this comparison we chose, for each stellar model, the mass cut that provides the ejection of the same amount of  $^{56}\text{Ni}$ , as in the corresponding WW95 model. Note that, since the grid of metallicities computed by WW95 does not coincide exactly with those presented here, the comparison shown in Figure 3

refers to models having a slightly different initial metallicity. We selected 20 and 25  $M_{\odot}$  because those dominate the yields of a stellar generation having a Salpeter-like IMF (see, e.g., LC03). Figure 3 (bottom right panel) shows that there is very good agreement between our and the WW95 yields for 25  $M_{\odot}$  of solar metallicity. On the contrary, all other panels disclose significant (and not systematic!) differences between the two sets of yields. In particular, there are a few things worth noting: (1) both sets of models produce O and C in similar amounts (within a factor of 2), while the N yields tend to be similar only for  $Z \geq 10^{-3}$ ; (2) the light elements Ne, Na, and Mg tend to be significantly more produced in our models than in the WW95 ones, while Al is produced in quite similar amounts; (3) we tend to systematically underproduce the products of the explosive oxygen burning and incomplete Si burning, i.e., Si, S, Ar, and Ca, by roughly a factor of 2 with respect to WW95 (even if the relative scaling among these elements is remarkably similar); (4) additionally, the odd elements P, Cl, and K, tend to be quite largely underproduced in our models with respect to WW95; and (5) the iron peak nuclei show a quite contradictory behavior, because while Ti is always in good agreement, Co and Ni are generally overproduced, and Sc is often underproduced relative to WW95.

A proper understanding of the sources of such differences, although of overwhelming interest, is extremely difficult

because the chemical yields are, in general, the result of a complex interplay among the various hydrostatic evolutionary phases plus the subsequent passage of the shock wave (Chieffi et al. 2000). For example, elements like N and Mg are not significantly affected by the passage of the shock wave, and hence their final differences will mainly reflect a different presupernova evolution (but note that, e.g., O, which it is also a product of the hydrostatic burnings, is produced in a very similar amount). Other elements are produced vice versa, by the explosive burnings, and therefore one could think that playing with the mass cut could significantly improve the comparison. This is not the case. First, note that the mass cut must be located within the region undergoing complete explosive Si burning, because appreciable amounts of Sc, Co, and Ni must be ejected. Hence, the abundances of the elements produced by explosive oxygen burning and/or incomplete explosive Si burning (Si, S, Ar, K, Ca, V, Cr, and Mn) would not be modified by changing the mass cut. Additionally, however, the comparison of the elements mainly produced by the complete explosive Si burning would not be improved by a changing of the mass cut, because a better fit to any of the elements like Sc, Ti, Co, and Ni would worsen the fit to the others.

A deeper comparison between these two sets is virtually impossible, because the two sets of models have been computed by adopting different choices for both the treatment of the convective layers and the rate of the  $^{12}\text{C}(\alpha, \gamma)^{16}\text{O}$  nuclear process and also because the models on which the WW95 yields are based have never been published. The only possible comparisons between our presupernova models and the ones that are at the base of the WW95 yields have been

presented in Limongi et al. (2000), and hence we refer the reader to that paper for such a comparison.

The differences between the WW95 and our yields are large enough that they should produce visible differences in GCE simulations, and hence we strongly suggest using both sets of yields in the GCE modeling to understand how alternative sets of yields influence our current understanding of the chemical evolution of the universe.

In conclusion, we provide in this paper a brand new set of yields in a wide range in both mass and initial metallicity. All the yields are freely available to the community for any choice of the mass cut (on request). We have shown for the first time that the initial chemical composition does not significantly affect the final yields up to at least a metallicity of the order of  $Z = 10^{-4}$ . We have also shown that a metallicity larger than  $Z = 10^{-3}$  is necessary to begin to produce elements beyond Zn up the neutron magic number  $N = 50$ . The present yields are quite different from those of WW95, and the observed differences cannot be simply explained in terms of one or a few causes but are certainly due to the complex interplay among various aspects of both the hydrostatic evolution and the explosion itself, which are very difficult to disentangle at the moment.

A. C. warmly thanks John Lattanzio and Brad Gibson for their kind hospitality in Melbourne and for providing the computer facilities (the Australian Partnership for Advanced Computing National Facility and the Swinburne Centre for Astrophysics and Supercomputing in Melbourne) necessary to perform such a huge number of computations.

#### REFERENCES

- Anders, E., & Grevesse, N. 1989, *Geochim. Cosmochim. Acta*, 53, 197  
 Arnett, D. 1996, *Supernovae and Nucleosynthesis* (Princeton: Princeton Univ. Press)  
 Bazan, G., & Arnett, D. 1994, *ApJ*, 433, L41  
 Chieffi, A., & Limongi, M. 2002, *ApJ*, 577, 281  
 Chieffi, A., Limongi, M., & Straniero, O. 1998, *ApJ*, 502, 737  
 ———. 2000, in *The Evolution of the Milky Way*, ed. F. Matteucci & F. Giovannelli (Dordrecht: Kluwer), 403  
 Chiosi, C., & Maeder, A. 1986, *ARA&A*, 24, 329  
 Heger, A., Langer, N., & Woosley, S. E. 2000, *ApJ*, 528, 368  
 Imbriani, G., Limongi, M., Gialanella, L., Terrasi, F., Straniero, O., & Chieffi, A. 2001, *ApJ*, 558, 903  
 Limongi, M., & Chieffi, A. 2002, *Publ. Astron. Soc. Australia*, 19, 246  
 ———. 2003, *ApJ*, 592, 404  
 Limongi, M., Straniero, O., & Chieffi, A. 2000, *ApJS*, 129, 625  
 Maeda, K., & Nomoto, K. 2003, *ApJ*, 598, 1163  
 Mezzacappa, A., & Bruenn, S. W. 1993, *ApJ*, 405, 669  
 Richtmeyer, R., & Morton, K. 1967, *Difference Methods for Initial Value Problems* (New York: Wiley)  
 Thielemann, F. K., Nomoto, K., & Hashimoto, M. 1996, *ApJ*, 460, 408  
 Timmes, F. X., Woosley, S. E., & Weaver, T. A. 1995, *ApJS*, 98, 617 (TWW95)  
 Weaver, T. A., & Woosley, S. E. 1993, *Phys. Rep.*, 227, 65  
 Woosley, S. E., & Weaver, T. A. 1988, *Phys. Rep.*, 163, 79  
 ———. 1995, *ApJS*, 101, 181 (WW95)